Silicon carbide monolayer with alkali and alkaline earth metal adatoms for H_2 storage: a computational study

Francisco de Santiago[a], Lucía Arellano[b], Álvaro Miranda[c], Fernando Salazar[d], Luis A. Pérez[e] and Miguel Cruz-Irisson[f]

[a] *Instituto Politécnico Nacional, ESIME-Culhuacán, Av. Santa Ana 1000, C.P. 04440, Ciudad de México, México, fdesantiagov0900@alumno.ipn.mx* ***CA***
[b] *Instituto Politécnico Nacional, ESIME-Culhuacán, Av. Santa Ana 1000, C.P. 04440, Ciudad de México, México, lucia.arellano.gin2017@gmail.com*
[c] *Instituto Politécnico Nacional, ESIME-Culhuacán, Av. Santa Ana 1000, C.P. 04440, Ciudad de México, México, amirandad.ipn@gmail.com*
[d] *Instituto Politécnico Nacional, ESIME-Culhuacán, Av. Santa Ana 1000, C.P. 04440, Ciudad de México, México, fsalazarp@ipn.mx*
[e] *Instituto de Física, Universidad Nacional Autónoma de México, Apartado Postal 20-364, 01000 Ciudad de México, México, lperez@fisica.unam.mx*
[f] *Instituto Politécnico Nacional, ESIME-Culhuacán, Av. Santa Ana 1000, C.P. 04440, Ciudad de México, México, irisson.ipn@gmail.com*

Abstract:

Given their great surface-to-volume ratio, bidimensional monolayers are ideal for hydrogen storage in fuel cell systems. It has been demonstrated that the silicon carbide (SiC) monolayer has a sp^2 hybridization which makes it an alternative to graphene. In this work, the hydrogen adsorption properties of a silicon carbide monolayer decorated with alkali and alkaline earth metal atoms are analysed by means of first-principles calculations. The results suggest that the adatoms cause little distortion to the monolayer, and they tend to be adsorbed on sites above Si atoms. The adatoms act as adsorption sites for H_2 molecules: up to seven molecules can be adsorbed by K, Mg and Ca. The adsorption energies suggest that H_2 molecules are physisorbed over the decorated SiC monolayer, which means that no chemical bonds are created between H_2 and the adatoms. This is beneficial because the breaking of chemical bonds, which would be needed to make use of the stored H_2, is energetically expensive. These results add to a continuing effort to develop efficient means of reversible hydrogen storage.

Keywords:

2D materials, Alkali metals, Density Functional Theory, Hydrogen storage, Silicon carbide.

1. Introduction

Silicon carbide has attracted much interest due to its useful properties: resistance to corrosion, large band gap (3.2 eV), high mechanical strength, low density, high hardness, high thermal conductivity

and low thermal expansion coefficient (1–3). Several theoretical studies have investigated the atomic structure and electronic properties of nanostructured SiC as a promising material for the next generation of nanoelectronics and energy applications (4); for example, nanoporous SiC (5–7), nanotubes for energy storage (8) or nanowires for optoelectronics (9–11). Nanostructured SiC has also been synthesized as nanohole arrays (12), nanowires for piezoelectronics (13) or thin films for thermal sensors (14).

Among the different nanoscale structures that can be investigated, 2D materials have been given extensive attention in recent years since the rise of graphene. A number of applications have been found for this type of materials, including p−n junctions and transistors (15,16), gas sensors (17,18), spintronics (19), components for Li−ion and Na−ion batteries (20), and so on. Similar to graphene in its honeycomb structure, sp^2 bonding and flatness (21), a SiC monolayer could exhibit a large band gap and benefit from the advantageous properties of SiC, while having the potential applications in which 2D materials excel. At the time of writing, ultrathin SiC nanoflakes and nanosheets have been successfully synthesized (15,22,23).

The study of the adsorption mechanisms of H_2 on solid-state materials is essential for the widespread adoption of hydrogen as an energy carrier, which has been demonstrated to be cleaner and more available than fossil fuels (24,25). Storage by solid state materials provides advantages over compressed gas or liquefaction, which would require great quantities of energy to produce the appropriate temperatures and pressures (25). The nanostructuring of materials greatly extends their usable surface area per volume unit, and this improves their adsorption properties (26,27). This application relies on the ability of the host material to adsorb H_2 molecules, although a strong bonding is not favourable since it would make difficult the cleaning and reuse of the host material.

H_2 adsorption can be achieved using functionalizing atoms deposited on a substrate (28–30). Transition metals have been used in several materials, however, clustering of these atoms tends to happen, which hinders the adsorption of H_2 molecules (31–33).

Given the potential advantages of a SiC monolayer, we propose it as a possible substrate for the storage and detection of molecular hydrogen. To avoid the use of transition metals, we explore the potential use of alkali and alkaline-earth metal atoms decorating the monolayer as H_2 adsorption sites. Besides preventing the formation of metal clusters, the use of alkali and alkaline-earth metals would reduce the weight of the storage system and increase its gravimetric capacity. A recent work (34) reported the adsorption of alkali and alkaline metals on a SiC monolayer by means of DFT. The work described the possibility of hydrogen and oxygen evolution reactions using free energy calculations. Another paper (35) explored the cases of Li- and Ca-decorated SiC monolayers. However, a systematic study of the capacity of metal-decorated SiC monolayers to adsorb a number of H_2 molecules, as has been carried out for graphene (36) or silicene (29), is still absent from the literature.

In this paper, the properties of the pristine SiC monolayer are first obtained. Subsequently, an alkali or alkaline-earth metal atom is placed on different possible adsorption sites on a SiC monolayer supercell, and the most favourable site is chosen. On this site, from 1 to 7 hydrogen molecules are placed, to evaluate the adsorption on the monolayer and how it is affected by the number of H_2 molecules in the proximity. For comparison, the possible case of a H_2 molecule adsorbed on the pristine SiC monolayer is also calculated.

2. Computational details

Density Functional Theory (37,38) was used to calculate the total energy of all systems, by means of the SIESTA method (39). Exchange and correlation potentials were calculated through the PBE functional (40), within the GGA approximation. A double-ζ polarized basis set was used (41,42), as well as Troullier-Martin's norm-conserving pseudopotentials (43) in a fully non-local form (44). The real space grid for numerical integrations was defined by a cut-off energy of 460 Ry. A reciprocal-space grid of 24×24×1 was generated by the Monkhorst-Pack technique (45). Atomic structures were optimized using a conjugate gradient algorithm, as implemented in the SIESTA

code, until the force between any pair of atoms was less than 0.001 eV/Å. To calculate the resulting electronic charge correspondent to each atom, and evaluate their gain or loss of electrons, Voronoi electronic population analysis was employed (46).

The decorated monolayers with a variating number of H_2 molecules were all modelled in a 5×5 SiC-monolayer supercell. Periodic boundary conditions are used, and to avoid unwanted interactions, a distance of 10 Å separates the monolayer from its artificial image along its z direction.

3. Results and discussion

As the first step, the pristine SiC monolayer is geometrically optimized. Its structural characteristics are shown in Fig. 1. The Si–C bond length is 1.8 Å, while the lattice parameter is 3.11 Å. As with graphene, sp^2 hybridization allows the structure to be flat, unlike silicene and other 2D materials. This structure is a semiconductor with a band gap of 2.04 eV, the corresponding density of states is shown in Fig. 2. These values are close to those reported in the literature with more expensive calculation techniques (34).

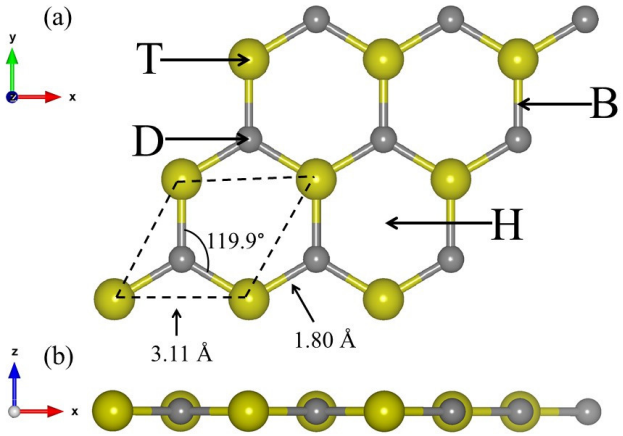

Figure 1. (a) Top view of a fragment of the SiC monolayer. T, D, H and B are adsorption sites. The primitive cell is marked by dashed lines. (b) Side view of the fragment.

There are various adsorption sites for the metal atoms (see Fig. 1). On the optimized pristine SiC monolayer, a metal atom is placed in each of the sites and the system is geometrically optimized, to evaluate the most energetically favourable site for metal adsorption. Table 1 summarizes the results for each metal. The adsorption energy is calculated according to the next formula:

$$E_a = E_M + E_{SiC} - E_{SiC+M}, \quad (1)$$

where E_M is the total energy of an isolated metal atom, E_{SiC} is the total energy of the pristine SiC monolayer supercell, and E_{SiC+M} is the total energy of the optimized system of the monolayer supercell with the decorating metal atom. The adsorption energies fall in the range of chemisorption (47), that is, all metal atoms are bonded to the SiC monolayer, except for the Mg atom, which has an adsorption energy under 0.5 eV, and a very low charge transfer to the monolayer. The most favourable site for all metals was the T site, over a Si atom, which concurs with the site found by Baierle et al. (34) and Song et al. (35). The reason for this preference may arise from the known fact that, in the Si—C bonds, C tends to strongly attract the electronic cloud from the Si, given its larger electronegativity. The Si is thus ionized and creates a positively charged region which electrostatically attracts the electronic cloud from the metals. Moreover, the Si atoms on the SiC monolayer have an open p-shell, which can readily accommodate one electron to complete the octet.

Table 1. Results for adsorption of metal atoms on each site of the monolayer: adsorption energies (E_a), metal-monolayer distance (h) and charge transfer from the metal atom (Q_V).

Metal	Site	E_a (eV)	h (Å)	Q_V ($\|e\|$)
Li	B	1.23	2.74	0.41
	T	1.23	2.74	0.41
	D	0.86	2.67	0.38
	H	1.23	2.54	0.41
Na	B	0.88	2.75	0.48
	T	0.88	2.76	0.48
	D	0.63	2.95	0.36
	H	0.72	2.78	0.39
K	B	1.01	3.15	0.51
	T	1.01	3.15	0.51
	D	0.84	3.03	0.51
	H	1.01	3.15	0.51
Be	B	0.25	2.84	0.10
	T	0.68	2.18	0.30
	D	0.15	3.58	0.03
	H	0.29	3.05	0.04
Mg	B	0.31	3.19	0.10
	T	0.31	3.18	0.10
	D	0.30	3.68	0.04
	H	0.31	3.29	0.05
Ca	B	0.60	3.01	0.47
	T	0.60	3.01	0.47
	D	0.36	3.81	0.15
	H	0.36	3.56	0.08

The adsorption of the metal causes a small displacement out of the plane of the Si atom below, but otherwise the monolayer has no important distortion. The calculation of the partial density of states (see Fig. 2) for each of the metal-decorated shows that in all cases there are occupied states with contribution from the metal and Si, which suggests a hybridization of atomic orbitals and the possible formation of a chemical bond. This is favourable because this atom will serve as adsorption centre for H_2 molecules. All the structures are semiconductors.

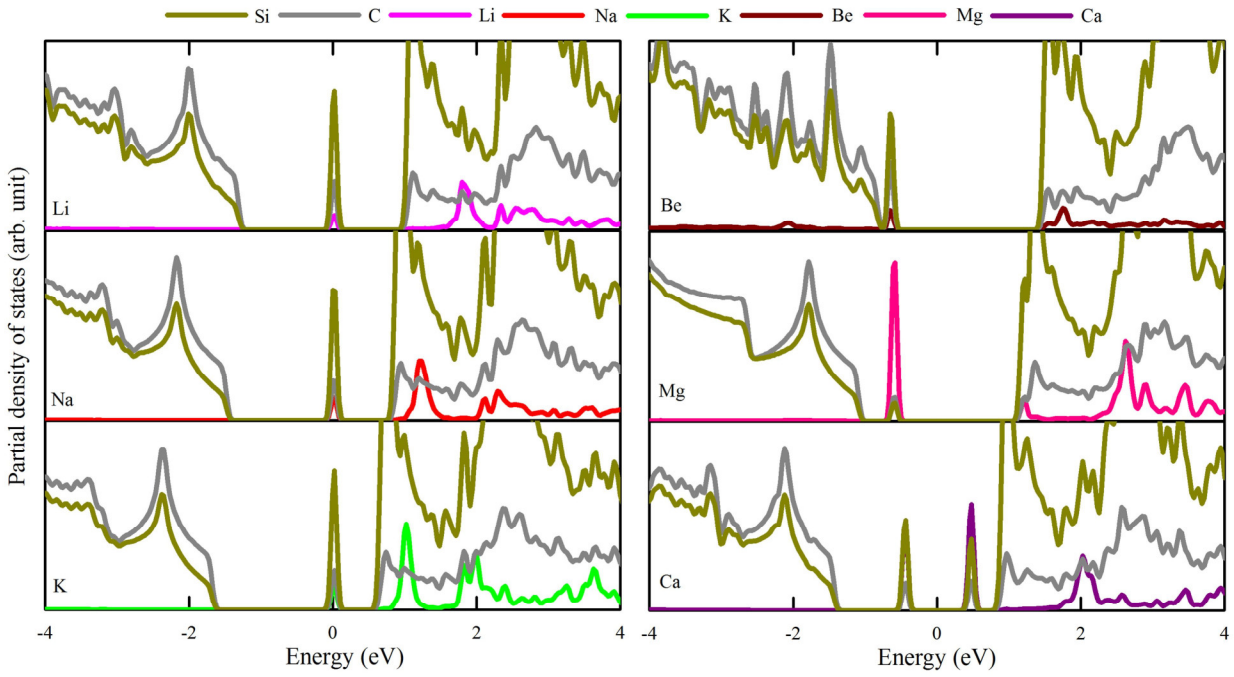

Figure 2. Partial densities of states of the alkali and alkaline-earth metals-decorated monolayer. The Fermi level is set to zero.

The possibility of the metal atoms clustering, which would be detrimental to the hydrogen storage capacity of the monolayer, is evaluated by comparing the adsorption energy of each metal to the SiC with the cohesive energy of each metal in its stable bulk form (48) (see Fig. 3). If the bulk cohesive energy is larger, the metal atoms prefer to bond together than disperse evenly on the monolayer, which may cause the creation of metal clusters. In the opposite case, the single metal atoms tend to be dispersed through the monolayer. Our results are compared with those obtained theoretically for silicene and graphene (29), showing that the only case in which the cohesive bulk energy is smaller is that of K. The monolayer-metal binding energies lie between graphene and silicene, but in all cases, values for silicene are more than 100% larger.

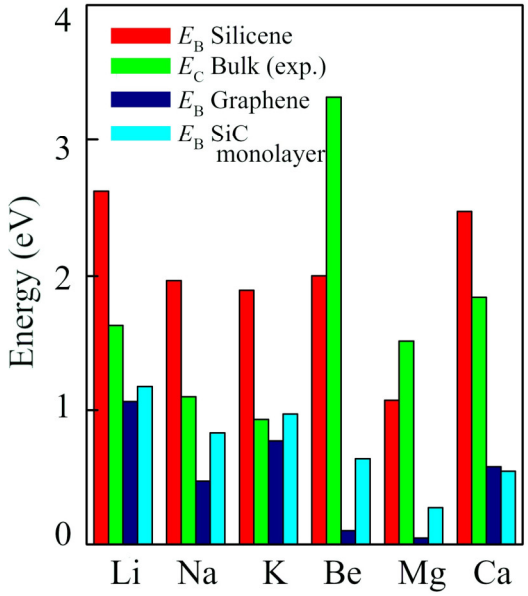

Figure 3. Comparison of calculated metal binding energies on SiC monolayer (BE SiC), with the cases of graphene (BE Graphene), silicene (BE Silicene), and the experimental cohesive energies (CE) of the bulk alkali and alkaline-earth metals.

Now we turn to the analysis of the interaction between H_2 and the pristine SiC monolayer. We carried out the tests for the most stable adsorption site for H_2, and for the most favourable position: a case where the molecular axis is perpendicular to the monolayer plane, and a case where it is parallel. This is evaluated using the next equation for the adsorption energy:

$$E_a = E_H + E_{SiC} - E_{SiC+H}, \quad (2)$$

where E_H is the total energy of a hydrogen molecule, E_{SiC} is the total energy of the pristine SiC monolayer supercell, and E_{SiC+H} is the total energy of the optimized system of the monolayer supercell with a hydrogen molecule. The results are shown on Table 2. The preferred site is the H, and the preferred orientation is perpendicular. The partial densities of states of the pristine and the H_2-adsorbed monolayers is shown in Fig. 4. The states from H are concentrated around 6 and -6 eV and cause only a small change in the curves of Si and C, which means that a chemical bond between the molecule and the monolayer is unlikely. Although the adsorption energy is in the range of physisorption, only one H_2 molecule can be adsorbed in the H site on the pristine monolayer.

Table 2. Results for adsorption of one H_2 molecule on the pristine monolayer: adsorption energies (E_a), molecule-monolayer distance (h) and charge transfer from the molecule (Q_V).

H_2 orientation	Site	E_a (eV)	h (Å)	Q_V ($\|e\|$)
Perpendicular	B	0.11	2.78	0.05
	T	0.10	2.83	0.05
	D	0.11	2.76	0.05
	H	0.13	2.50	0.05
Parallel	B	0.11	2.79	0.04
	T	0.10	2.94	0.07
	D	0.12	2.61	0.06
	H	0.12	2.60	0.05

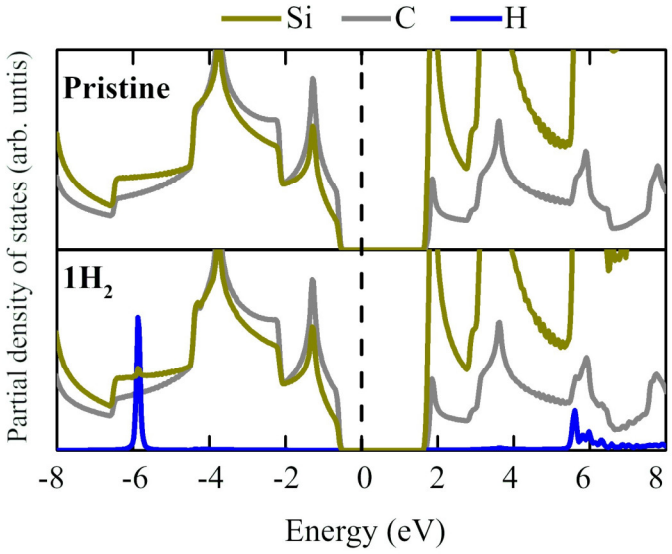

Figure 4. Partial densities of states of the pristine and H_2-adsorbed on pristine SiC monolayer.

Once the preferred site was found, more H_2 molecules were added to see the maximum number of molecules each decorated monolayer can adsorb before the adsorption strength is too weak, or the molecules are too far away from the metal. For this analysis, the adsorption energy was calculated with the following formula:

$$E_a = NE_H + E_{SiC+M} - E_{SiC+M+H}, \quad (3)$$

where E_H is the total energy of a hydrogen molecule, N is the number of hydrogen molecules on the model, E_{SiC+M} is the total energy of the pristine SiC monolayer supercell with a decorating atom, and $E_{SiC+M+H}$ is the total energy of the optimized system of the decorated monolayer supercell with N hydrogen molecules. Table 3 summarizes the results for the calculation with several hydrogen atoms, showing only the results before the hydrogen molecules are too far away or are adsorbed to other H sites with no metal atom.

Table 3. Results for adsorption of N hydrogen molecules on the decorated monolayer: adsorption energies (E_a), average molecule-metal distance (h) and average charge transfer from the molecules to the decorated SiC monolayer (Q_V).

Metal	N	E_a (eV)	h (Å)	Q_V ($\|e\|$)
Li	1	0.26	2.42	0.20
	2	0.29	2.46	0.28
	3	0.29	2.47	0.38
Na	1	0.16	2.74	0.19
	2	0.23	2.76	0.28
	3	0.24	2.76	0.40
	4	0.31	2.78	0.40
K	1	0.13	3.12	0.20
	2	0.22	3.13	0.30
	3	0.22	3.14	0.45
	4	0.22	3.15	0.47
	5	0.20	3.15	0.50
	6	0.20	3.17	0.53
	7	0.19	3.17	0.57
Be	1	0.17	2.19	0.17
Mg	1	0.01	3.11	0
	2	0.12	3.11	0
	3	0.12	3.10	0
	4	0.13	3.10	0
	5	0.13	3.08	0.01
	6	0.13	3.08	0.02
	7	0.13	3.08	0.02
Ca	1	0.02	3.02	0.03
	2	0.13	3.02	0.10
	3	0.13	3.02	0.18
	4	0.15	2.96	0.48
	5	0.16	2.99	0.58
	6	0.16	3.01	0.64
	7	0.16	3.01	0.67

Li- and Be-decorated monolayers have low adsorption capacity, owing probably to their small size. These results agree with other reports on bidimensional SiC (35) and silicene (29). Adsorption on the K-, Mg- and Ca-decorated monolayers is maximum, achieving up to 7 molecules. However, Mg decoration is weak, as shown on Table 1. The results of the Ca-decorated monolayer agree with Song et al. (35), although we found weaker adsorptions. The major capacity with strongest adsorption was found in the case of K, which also showed low electronic charge transfer, which may suggest that, although the molecules are strongly adsorbed on the decorated monolayer, there is no chemical bonding, in other words, the molecules are only physisorbed on the monolayer, and it

will be readily possible to desorb them in order to feed a fuel cell. The H—H bonds were not broken for the H_2 concentrations reported, all of them being 0.79 Å. On Fig. 5 the partial densities of states of the K-decorated monolayer with an increasing number of molecules are plotted. The contribution of H below the Fermi level is centered around -8.5 eV, and these contributions does not modify the Si and C curves as the number of H grows. This evidences the absence of orbital hybridization, and thus chemical bonds, between the H and the atoms of the monolayer.

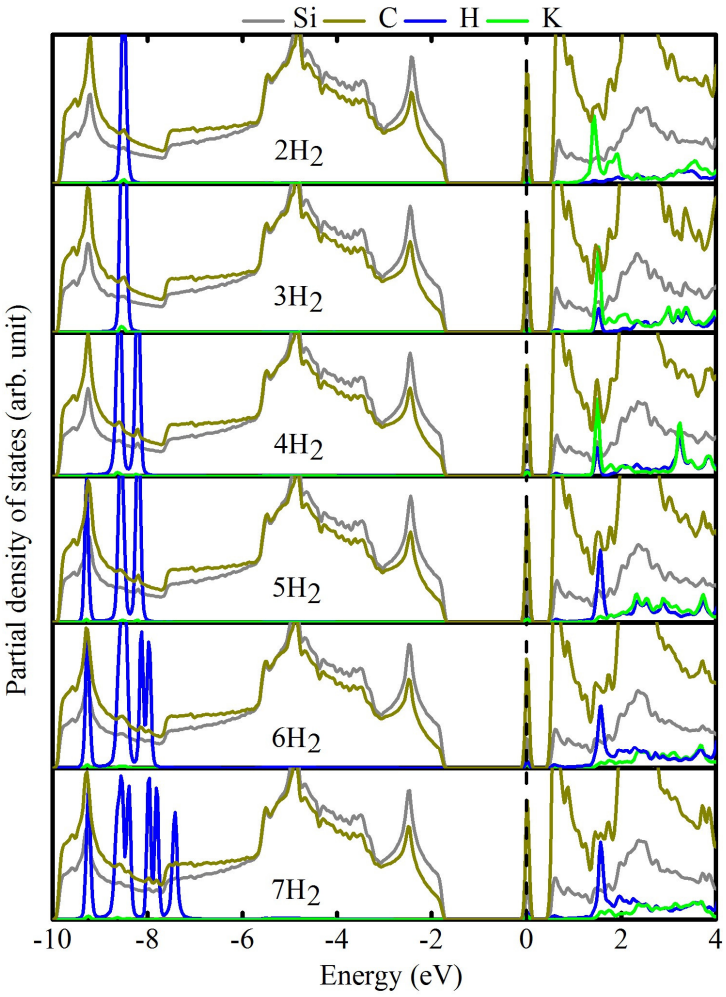

Figure 5. Partial densities of states of the K-decorated SiC monolayer, with an increasing number of H_2 molecules (1 to 7).

4. Conclusions

In this work, the capacity of SiC honeycomb, graphene-like, monolayers decorated with alkali and alkaline-earth metal atoms to physisorb H_2 molecules has been investigated using Density Functional Theory. It was found that alkali and alkaline-earth metals can be chemisorbed on the SiC monolayer, except for Mg, which is physisorbed. The preferred site for the adsorption of metals is the Top (T) site, above a Si atom. While only one H_2 molecule can be adsorbed by the pristine SiC monolayer, the metal-decorated SiC monolayer can adsorb up to 7 molecules (the case of K and Ca adatoms) before the molecules start to be too far from the adatom and adsorb on adjacent H sites. From the perspective of efficient hydrogen storage, the K-decorated SiC monolayer would be the optimal option, as it is the lightest adatom that achieved the largest capacity with reasonably strong adsorption energy. Moreover, it was estimated that only K would avoid clustering over the SiC monolayer. Is important to note that Baierle et al. (34) have recently investigated the adsorption of alkali and alkaline-earth atoms on SiC monolayers, and its possible reaction with a H and O atom. Our results are in excellent agreement with theirs, which were calculated using the VASP code for

DFT, with PAW pseudopotentials and a hybrid exchange-correlation functional. We hope that these results contribute to the ongoing search for ways to engineer materials with desirable properties for clean energy generation and storage.

Acknowledgments

This work was partially supported by multidisciplinary projects IPN-SIP 2018-1937 and 2018-1969, individual project IPN-SIP 2019-5830, and UNAM-PAPIIT IN107717. Computations were performed at the supercomputer Miztli of DGTIC-UNAM (Project LANCAD-UNAM-DGTIC-180), at supercomputer Abacus-I of CINVESTAV-EDOMEX, and at the supercomputer Xiuhcóatl of CINVESTAV (Project LANCAD). F.S. and L.G.A. would like to thank BEIFI-IPN, CONACYT and COFAA-IPN for their financial support. The authors wish to acknowledge the contribution of José A. Galicia for the conception and the early development stages of this work.

References

[1] Ivanov PA, Chelnokov VE. Recent developments in SiC single-crystal electronics. Semicond Sci Technol. 1992;7(7):863–80.

[2] Janzen E, Henry A, Chen WM, Son NT, Monemar B, Sorman E, et al. SiC - A Semiconductor for High-Power , High-Temperature and High- Frequency Devices. Phys Scripta. 1994;54:283–90.

[3] Casady JB, Johnson RW. Status of silicon carbide (SiC) as a wide-bandgap semiconductor for high-temperature applications: A review. Solid State Electron 1996;39(10):1409–22.

[4] Wu R, Zhou K, Yue CY, Wei J, Pan Y. Recent progress in synthesis, properties and potential applications of SiC nanomaterials. Prog Mater Sci 2015;72:1–60.

[5] González I, Trejo A, Calvino M, Miranda A, Salazar F, Carvajal E, M. Cruz-Irisson. Effects of surface and confinement on the optical vibrational modes and dielectric function of 3C porous silicon carbide: An ab-initio study. Phys B Condens Matter 2018;550:420–7.

[6] Tuttle BR, Held NJ, Lam LH, Zhang YY, Pantelides ST. Properties of hydrogenated Nanoporous SiC: An Ab initio study. J Nanomater. 2017;2017:4705734.

[7] Calvino M, Trejo A, Crisóstomo MC, Iturrios MI, Carvajal E, Cruz-Irisson M. Modeling the effects of Si-X (X = F, Cl) bonds on the chemical and electronic properties of Si-surface terminated porous 3C-SiC. Theor Chem Acc. 2016;135(4):104.

[8] Tabtimsai C, Ruangpornvisuti V, Tontapha S, Wanno B. A DFT investigation on group 8B transition metal-doped silicon carbide nanotubes for hydrogen storage application. Appl Surf Sci 2018;439:494–505.

[9] Li YJ, Li SL, Gong P, Li YL, Fang XY, Jia YH, Cao MS. Inhibition of quantum size effects from surface dangling bonds: The first principles study on different morphology SiC nanowires. Phys B Condens Matter 2018;539(January):72–7.

[10] Cuevas JL, de Santiago F, Ramírez J, Trejo A, Miranda Á, Pérez LA, Cruz-Irisson M. First principles band gap engineering of [1 1 0] oriented 3C-SiC nanowires. Comput Mater Sci. 2018;142:268–76.

[11] Miranda A, Cruz-Irisson M, Perez LA. Controlling stability and electronic properties of small-diameter SiC nanowires by fluorination. Int J Nanotechnol. 2015;12(3–4):218–25.

[12] Zhao L, Chen S, Wang L, Gao F, Yao X, Yang W. Large-scale fabrication of free-standing and transparent SiC nanohole array with tailored structures. Ceram Int. 2018;44(6):7280–5.

[13] Li X, Chen S, Ying P, Gao F, Liu Q, Shang M, Yang W. A giant negative piezoresistance effect in 3*C*-SiC nanowires with B dopants. J Mater Chem C. 2016;4(27):6466–72.

[14] Dinh T, Phan HP, Nguyen TK, Balakrishnan V, Cheng HH, Hold L, Lacopi A, Nguyen N-T, Dao DV. Unintentionally Doped Epitaxial 3C-SiC(111) Nanothin Film as Material for Highly

Sensitive Thermal Sensors at High Temperatures. IEEE Electron Device Lett. 2018;39(4):580–3.

[15] Lin SS. Light-emitting two-dimensional ultrathin silicon carbide. J Phys Chem C. 2012;116(6):3951–5.

[16] Frisenda R, Molina-Mendoza AJ, Mueller T, Castellanos-Gomez A, Van Der Zant HSJ. Atomically thin p-n junctions based on two-dimensional materials. Chem Soc Rev. 2018;47(9):3339–58.

[17] Liu X, Ma T, Pinna N, Zhang J. Two-Dimensional Nanostructured Materials for Gas Sensing. Adv Funct Mater. 2017;27(37):1–30.

[18] Choi SJ, Kim ID. Recent Developments in 2D Nanomaterials for Chemiresistive-Type Gas Sensors. Electron Mater Lett. 2018;14(3):221-60.

[19] Feng YP, Shen L, Yang M, Wang A, Zeng M, Wu Q, Chintalapati S, Chang C-R. Prospects of spintronics based on 2D materials. Wiley Interdiscip Rev Comput Mol Sci. 2017;7(5):e1313.

[20] Shi L, Zhao T. Recent advances in inorganic 2D materials and their applications in lithium and sodium batteries. J Mater Chem A. 2017;5(8):3735–58.

[21] Bekaroglu E, Topsakal M, Cahangirov S, Ciraci S. First-principles study of defects and adatoms in silicon carbide honeycomb structures. Phys Rev B - Condens Matter Mater Phys. 2010;81(7):1–9.

[22] Chabi S, Chang H, Xia Y, Zhu Y. From graphene to silicon carbide: Ultrathin silicon carbide flakes. Nanotechnology. 2016;27(7):075602.

[23] Susi T, Skákalová V, Mittelberger A, Kotrusz P, Hulman M, Pennycook TJ, . Computational insights and the observation of SiC nanograin assembly: Towards 2D silicon carbide. Sci Rep. 2017;7(1):4399.

[24] Gaudernack B, Lynum S. Hydrogen from natural gas without release of CO_2 to the atmosphere. Int J Hydrogen Energy. 1998;23(12):1087–93.

[25] Niaz S, Manzoor T, Pandith AH. Hydrogen storage: Materials, methods and perspectives. Renew Sustain Energy Rev. 2015;50:457–69.

[26] Liu T, Ding J, Su Z, Wei G. Porous two-dimensional materials for energy applications: Innovations and challenges. Mater Today Energy 2017;6:79–95.

[27] Yu X, Tang Z, Sun D, Ouyang L, Zhu M. Recent advances and remaining challenges of nanostructured materials for hydrogen storage applications. Prog Mater Sci. 2017;88:1–48.

[28] Honarpazhouh Y, Astaraei FR, Naderi HR, Tavakoli O. Electrochemical hydrogen storage in Pd-coated porous silicon/graphene oxide. Int J Hydrogen Energy. 2016;41(28):12175–82.

[29] Wang Y, Zheng R, Gao H, Zhang J, Xu B, Sun Q, Jia Y. Metal adatoms-decorated silicene as hydrogen storage media. Int J Hydrogen Energy. 2014;39(26):14027–32.

[30] Du A, Zhu Z, Smith SC. Multifunctional Porous Graphene for Nanoelectronics and Hydrogen Storage: New Properties Revealed by First Principle Calculations. J Am Chem Soc. 2010;132(9):2876–7.

[31] Sun Q, Wang Q, Jena P, Kawazoe Y. Clustering of Ti on a C_{60} Surface and Its Effect on Hydrogen Storage. J Am Chem Soc. 2005;127(42):14582–3.

[32] Krasnov PO, Ding F, Singh AK, Yakobson BI. Clustering of Sc on SWNT and reduction of hydrogen uptake: Ab-initio all-electron calculations. J Phys Chem C. 2007;111(49):17977–80.

[33] Chakraborty B, Modak P, Banerjee S. Hydrogen storage in yttrium-decorated single walled carbon nanotube. J Phys Chem C. 2012;116(42):22502–8.

[34] Baierle RJ, Rupp CJ, Anversa J. Alkali (Li, K and Na) and alkali-earth (Be, Ca and Mg) adatoms on SiC single layer. Appl Surf Sci 2018;435:338–45.

[35] Song N, Wang Y, Zheng Y, Zhang J, Xu B, Sun Q, Jia Y. New template for Li and Ca decoration and hydrogen adsorption on graphene-like SiC: A first-principles study. Comput Mater Sci 2015;99:150–5.

[36] Pantha N, Belbase K, Adhikari NP. First-principles study of the interaction of hydrogen molecular on Na-adsorbed graphene. Appl Nanosci. 2015;5(4):393–402.

[37] Hohenberg P, Kohn W. Inhomogeneous Electron Gas. Phys Rev 1964;136(3B):B864–71.

[38] Kohn W, Sham LJ. Self-Consistent Equations Including Exchange and Correlation Effects. Phys Rev 1965;140(4A):A1133–8.

[39] Soler JM, Artacho E, Gale JD, García A, Junquera J, Ordejón P, Sánchez-Portal D. The SIESTA method for *ab initio* order-*N* materials simulation. J Phys Condens Matter 2002;14(11):2745.

[40] Perdew JP, Burke K, Ernzerhof M. Generalized Gradient Approximation Made Simple. Phys Rev Lett 1996 Oct 28;77(18):3865–8.

[41] Artacho E, Sánchez-Portal D, Ordejón P, García A, Soler JM. Linear-Scaling ab-initio Calculations for Large and Complex Systems. Phys status solidi 1999;215(1):809–17.

[42] Junquera J, Paz Ó, Sánchez-Portal D, Artacho E. Numerical atomic orbitals for linear-scaling calculations. Phys Rev B 2001;64(23):235111.

[43] Troullier N, Martins JL. Efficient pseudopotentials for plane-wave calculations. Phys Rev B 1991;43(3):1993–2006.

[44] Kleinman L, Bylander DM. Efficacious Form for Model Pseudopotentials. Phys Rev Lett 1982;48(20):1425–8.

[45] Monkhorst HJ, Pack JD. Special points for Brillouin-zone integrations. Phys Rev B. 1976;13(12):5188–92.

[46] Fonseca Guerra C, Handgraaf J-W, Baerends EJ, Bickelhaupt FM. Voronoi deformation density (VDD) charges: Assessment of the Mulliken, Bader, Hirshfeld, Weinhold, and VDD methods for charge analysis. J Comput Chem. 2004;25(2):189–210.

[47] Oura K, Katayama M, Zotov AV, Lifshits VG, Saranin AA. Surface Science. Springer; 2003.

[48] Kittel C. Introduction to Solid State Physics. Wiley; 2004.